RIMS Kôkyûroku Bessatsu
B31 (2012), 135–155

Coexistence of stable spots and fronts in a three-component FitzHugh–Nagumo system

Dedicated, with gratitude and deep respect, to Professor Yasumasa Nishiura on the occasion of his 60th birthday

By

Peter van Heijster* and Björn Sandstede**

Abstract

We investigate regions of bistability between different travelling and stationary structures in a planar singularly-perturbed three-component reaction-diffusion system that arises in the context of gas discharge systems. In previous work, we delineated the existence and stability regions of stationary localized spots in this system. Here, we complement this analysis by establishing the stability regions of planar travelling fronts and stationary stripes. Taken together, these results imply that stable fronts and spots can coexist in three-component systems. Numerical simulations indicate that the stable fronts never move towards stable spots but instead move away from them.

Received April 16, 2011.
2000 Mathematics Subject Classification(s): 35K57, 35B35, 35B25
Key Words: fronts, spots, three-component systems, coexistence
Van Heijster was supported by the Netherlands Organisation for Scientific Research (NWO). Sandstede was partially supported by the NSF through grant DMS-0907904. The authors are grateful to K.-I. Ueda for allowing them to use his numerical code and thank S.-I. Ei for asking questions about coexistence that led to this paper.
*Department of Mathematics and Statistics, Boston University, 111 Cummington Street, Boston, MA 02215, USA.
e-mail: heijster@math.bu.edu
**Division of Applied Mathematics, Brown University, 182 George Street, Providence, RI 02912, USA.
e-mail: bjorn_sandstede@brown.edu

§ 1. Introduction

We are interested in bistability between stable planar front and spot solutions in the context of the planar three-component reaction-diffusion system

$$\begin{aligned} u_t &= \epsilon^2 \Delta u + u - u^3 - \epsilon(\alpha v + \beta w + \gamma)\,, \\ \tau v_t &= \Delta v + u - v\,, \\ \theta w_t &= D^2 \Delta w + u - w \end{aligned} \tag{1.1}$$

that was proposed by Purwins [10, 11] as a phenomenological model for gas-discharge systems. Here, we will always take $x = (x_1, x_2) \in \mathbb{R}^2$, use the notation $U = (u, v, w)$, and assume that $D > 1$, $\tau, \theta > 0$, and $\alpha, \beta, \gamma \in \mathbb{R}$ are fixed independently of the positive parameter ϵ.

The dynamics of (1.1) for not necessarily small values of $\epsilon > 0$ has been studied previously in many papers through formal analyses and numerical simulations, and we refer to [4, 9, 10, 11, 12, 13] for representative works. Another work we wish to highlight is [8] in which Nishiura and his coworkers investigated the effect of head-on collisions of counterpropagating 1D pulses and radial 2D spots of (1.1): their results indicate that unstable stationary states of saddle type, termed scattors in [8], determine the fate of localized structures at collision. For general values of ϵ, not much can be said rigorously, and we therefore focus from now on on the regime $0 < \epsilon \ll 1$ where geometric singular perturbation theory can be used to analyse (1.1).

We begin by briefly discussing the properties of the homogeneous rest states that serve as the background states of the planar structures we will consider. The system (1.1) has precisely three stationary homogeneous solutions $U(x,t) = U_*^j := u_*^j(1,1,1)$ with $j = 0, \pm$, where $u_*^{\pm,0}$ denote the three roots

$$u_*^{\pm} = \pm 1 \mp \frac{1}{2}\epsilon(\alpha + \beta \pm \gamma) + \mathcal{O}(\epsilon^2)\,, \qquad u_*^0 = \epsilon\gamma + \mathcal{O}(\epsilon^2) \tag{1.2}$$

of the cubic polynomial $u^3 - u + \epsilon((\alpha + \beta)u + \gamma)$. The homogeneous rest state U_*^0 is always unstable with respect to (1.1) and will not be considered further.

Next, we describe the three different kinds of localized solutions $U(x,t)$ of (1.1), namely stationary spots, planar travelling fronts, and planar stripes, that we are interested in. Spots are time-independent radial solutions $U(x,t) = U^{\mathrm{sp}}(|x|)$ with $U^{\mathrm{sp}}(|x|) \to U_*^-$ as $|x| \to \infty$. Planar fronts can be taken to travel in the x_1-direction and therefore correspond to solutions of the form $U(x,t) = U^{\mathrm{fr}}(x_1 - ct)$ where $U^{\mathrm{fr}}(x_1)$ converges to $U_*^{\pm}$ as $x_1 \to \pm\infty$. Similarly, we may consider planar stripes, which are stationary solutions of the form $U(x,t) = U^{\mathrm{st}}(x_1)$ that converge to U_*^- as $x_1 \to \pm\infty$. For $0 < \epsilon \ll 1$, fronts will resemble a sharp interface that connects U_*^- and U_*^+; similarly, stripes will consist of a plateau with value U_*^+ that is separated by two sharp monotone interfaces from the

rest state U_*^-. In particular, we can measure the width of a stripe by the plateau length. We remark that spots and stripes that converge to U_*^+ can be obtained by multiplying the solutions U asymptotic to U_*^- and the associated parameter value γ by -1.

Planar front and stripe profiles depend only on x_1 and therefore satisfy the one-dimensional version of (1.1). Their existence and stability has been studied recently in [2, 3, 5] in the regime $0 < \epsilon \ll 1$, and we summarize their results in the following theorem.

Theorem 1.1 ([2, 3, 5]). *Fix $D > 1$, $\tau, \theta > 0$, and $\alpha, \beta, \gamma \in \mathbb{R}$. Equation (1.1) then has a travelling front $U^{\mathrm{fr}}(x_1 - ct)$ with speed $c \approx \frac{3}{\sqrt{2}}\gamma\epsilon^2$ that is stable with respect to 1D perturbations[1] for each $0 < \epsilon \ll 1$. Furthermore, if there is an $L > 0$ such that $\alpha \mathrm{e}^{-2L} + \beta \mathrm{e}^{-2L/D} = \gamma$, then (1.1) admits a planar stripe $U^{\mathrm{st}}(x_1)$ of width approximately equal to $2L$ for each $0 < \epsilon \ll 1$, and this stripe is stable with respect to 1D perturbations provided $\alpha \mathrm{e}^{-2L} + \frac{\beta}{D}\mathrm{e}^{-2L/D} > 0$.*

One consequence of the preceding result is that planar travelling fronts exist regardless of the values of the fixed parameters and that they are always stable with respect to small perturbations that depend only on x_1. The next theorem, which is the main result of this paper, gives conditions under which planar fronts are spectrally stable with respect to 2D perturbations associated with finite transverse wave numbers.

Theorem 1.2. *Fix $D > 1$, $\tau, \theta > 0$, and $\alpha, \beta, \gamma \in \mathbb{R}$ and pick any constant k_*, then the planar travelling front $U^{\mathrm{fr}}(x_1 - ct)$ of (1.1) given in Theorem 1.1 is spectrally stable for $0 < \epsilon \ll 1$ with respect to perturbations whose transverse wave number k satisfies $|k| < k_*$ provided $\alpha + \frac{\beta}{D} < \frac{2\sqrt{2}}{3}$.*

Note that we do not state a spectral stability result for perturbations with arbitrary large transverse wave numbers k. While we believe that Theorem 1.2 is true for each wave number k, a rigorous proof is technical, and we decided not to pursue this direction. If the planar front is spectrally stable with respect to all transverse wave numbers, then the results in [7] indicate that it is nonlinearly stable with respect to small perturbations in $H^2(\mathbb{R})$: the results in [7] are stated for diffusion matrices that are multiples of the identity but should carry over to the general case of positive diagonal diffusion matrices under the assumption of spectral stability.

In Figure 1, we compare the time evolution of a stable planar travelling front that travels to the left with the predictions of Theorems 1.1 and 1.2 using direct simulations of (1.1). To illustrate the stability predictions of Theorem 1.2, we plot in Figure 2 the evolution of stable and unstable planar fronts.

Having discussed our stability results for planar fronts, we now recall the existence and stability properties of planar spots from [6].

[1] That is, with respect to perturbations that depend only on x_1.

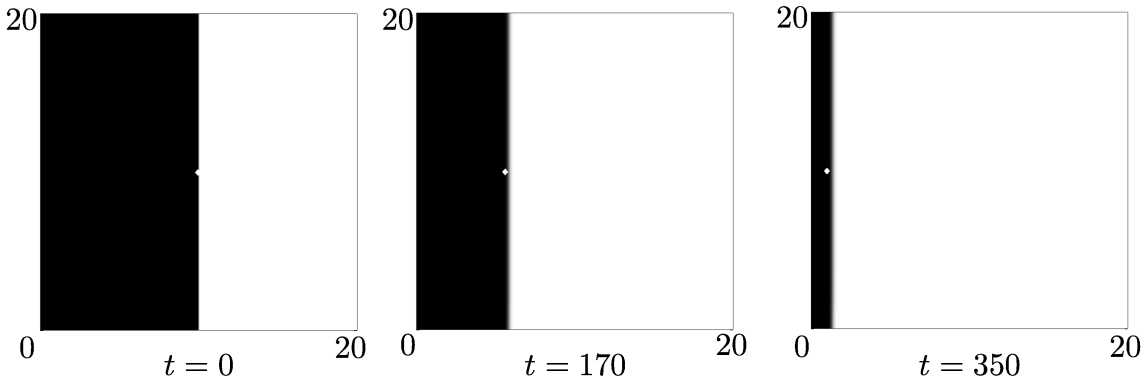

Figure 1. Shown are color plots of the u-profile of the stable planar travelling front of (1.1) at different times. Black corresponds to $u = u_*^-$, while white corresponds to $u = u_*^+$. The white diamond indicates the theoretically predicted position of the front at which the u-component vanishes. The parameter values are given in Table 1.

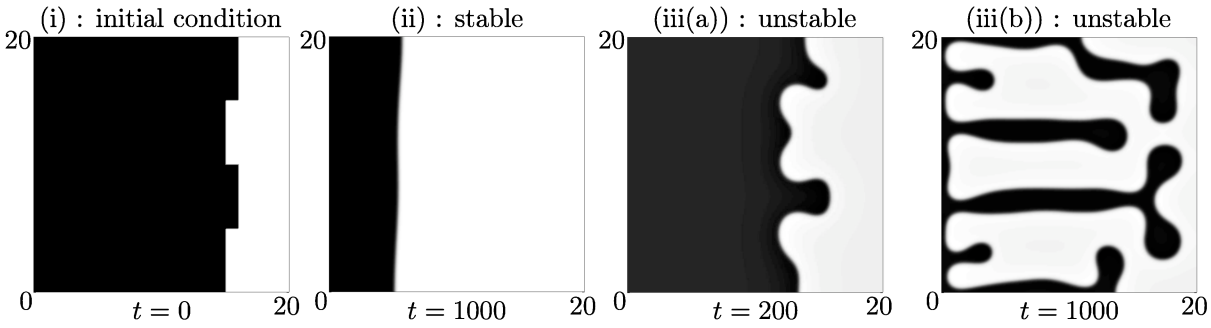

Figure 2. Plotted are color plots of the u-components of the initial condition in panel (i) and the emerging stable and unstable fronts in panels (ii) and (iii), respectively, for the two different sets of parameters given in Table 1. The front shown in panel (iii) is unstable for wave numbers $|k| < 1.93$ with $k = 1.13$ being the most unstable wave number.

Figure	α	β	γ	D	**Effect**
1	1	-0.5	-1.2	2	stable front
2 (ii)	1	-0.5	-0.5	2	slows down stable front
2 (iii)	3	-0.5	-0.5	2	destabilizes front
3	0.5	1	[-3.0, 0.5]	3	stable front interacts with spot
4	0.5	1	-0.5	3	two fronts move towards unstable spot
6	0.5	1	0.5	3	stable stationary pulse
7	0.5	1	0.5	3	stable stationary pulse and spot

Table 1. The table gives a summary of the parameter values used in our simulations and indicates the effects of parameter changes on the dynamics of spots and planar fronts. Throughout, we have $\epsilon = 0.1$, $\tau = 1$, and $\theta = 1$. We used a numerical code by Ueda [9] with a 5-point discretization of the Laplacian on a square of length 20 with 200 equidistant mesh points in each spatial direction and a semi-implicit scheme in time that uses conjugate gradients with incomplete Cholesky.

Theorem 1.3 ([6]). *Fix $D > 1$, $\tau, \theta > 0$, and $\alpha, \beta, \gamma \in \mathbb{R}$. Assume that $L > 0$ is a simple root of the function*[2]

$$R(L;\alpha,\beta,\gamma,D) := \frac{\sqrt{2}}{3L} + \alpha\Big(2LI_1(L)K_0(L) - 1\Big) + \beta\left(\frac{2L}{D} I_1\left(\frac{L}{D}\right) K_0\left(\frac{L}{D}\right) - 1\right) + \gamma\,, \tag{1.3}$$

then (1.1) admits a stationary radial spot solution $U^{\mathrm{sp}}(|x|)$ with width approximately equal to $2L$ for each $0 < \epsilon \ll 1$. If, in addition,

$$\lambda_n(L) = 3\sqrt{2}\alpha L\Big(I_1(L)K_1(L) - I_n(L)K_n(L)\Big) + 3\sqrt{2}\beta\frac{L}{D^2}\left(I_1\left(\frac{L}{D}\right)K_1\left(\frac{L}{D}\right) - I_n\left(\frac{L}{D}\right)K_n\left(\frac{L}{D}\right)\right) + \frac{1-n^2}{L^2} \tag{1.4}$$

is strictly negative for all integers n with $|n| \neq 1$, then the planar spot is spectrally, and therefore nonlinearly, stable with respect to small radial and non-radial perturbations.

The quantities $\lambda_n(L)$ in the preceding theorem correspond to the rightmost eigenvalues $\epsilon^2(\lambda_n(L)+\mathcal{O}(\epsilon))$ of the linearization about the spot that belong to eigenfunctions with angular wave number n. Spots can destabilize through Hopf ($|n| = 0, 2, 3, \cdots$) and drift ($|n| = 1$) bifurcations upon increasing the parameters τ and θ, and we currently

[2]The functions $I_j(z)$ and $K_j(z)$ are the modified Bessel functions of the first and second kind, respectively, with index j and argument z [1].

work on identifying parameter regimes where the drift bifurcation is supercritical and leads to stable travelling planar spots for (1.1).

We are now in a position to study the coexistence of stable spots and spectrally stable planar fronts by comparing the parameter regimes given in Theorem 1.2 and Theorem 1.3.

Corollary 1.4. *Fix $D > 1$, $\tau, \theta > 0$, and $\alpha, \beta, \gamma \in \mathbb{R}$ such that $\alpha + \frac{\beta}{D} < \frac{2\sqrt{2}}{3}$. If, in addition, (1.3) has a simple root $L > 0$ for which $\lambda_n(L)$ (1.4) is strictly negative for all integers n with $|n| \neq 1$, then a planar stable stationary spot and a travelling front coexist for all $0 < |\epsilon| \ll 1$. In particular, the point $(\alpha, \beta, \gamma, D, \tau, \theta) = (0.5, 1, 0.5, 3, 1, 1)$ is in the coexistence parameter regime.*

Thus, stable travelling fronts and stationary spots can coexist in three-component systems and may therefore interact. The numerical simulations shown below in Figure 3 suggest, however, that the stable front is always moving away from the stable stationary spot.

The remainder of this paper is organized as follows. In §2, we present a series of numerical simulations to illustrate the interaction dynamics of fronts, stripes, and spots. Section 3 is devoted to a proof of Theorem 1.2 via geometric singular perturbation theory.

§ 2. Interaction of fronts, stripes, and spots

We explore the dynamics of stable fronts and spots in the coexistence regime using numerical simulations. We also investigate the interaction of unstable structures that involve fronts, stripes, and spots. Finally, we analyse the existence and stability of planar stripes.

§ 2.1. Spot-front interaction

Corollary 1.4 implies that stable planar travelling fronts and stationary spots coexist in appropriate parameter regimes. It is then possible for these structures to interact through their tails, and we illustrate their interaction properties in Figure 3 using numerical simulations of (1.1). The system parameters $(\alpha, \beta, D, \tau, \theta, \epsilon) = (0.5, 1, 3, 1, 1, 0.1)$ are fixed during the numerical simulations, while we vary the forcing parameter γ between -3 and 0.5. For this range of parameter values, we have

$$\alpha + \frac{\beta}{D} = \frac{5}{6} < \frac{2\sqrt{2}}{3},$$

and Theorem 1.2 implies that there exists a stable traveling front $U^{\mathrm{fr}}(x_1 - ct)$ for these parameter values. Furthermore, this front moves to the right for $\gamma > 0$ and to the left

γ	front U^{fr}	spot U^{sp}
$\gamma < 0$	stable: moves to the left	one unstable spot
$0 < \gamma < 0.431$	stable: moves to the right	two unstable spots
$0.431 < \gamma < 0.653$	stable: moves to the right	one stable, one unstable spot
$0.653 < \gamma$	stable: moves to the right	no spots

Table 2. The table summarizes the results on existence, stability and velocity for traveling fronts $U^{\mathrm{fr}}(x_1 - ct)$ and stationary radial spots $U^{\mathrm{sp}}(|x|)$ for varying γ, see Theorems 1.2 and 1.3. The other parameters are kept fixed: $(\alpha, \beta, D, \tau, \theta, \epsilon) = (0.5, 1, 3, 1, 1, 0.1)$.

for $\gamma < 0$. On the other hand, Theorem 1.3 shows that a single unstable radial spot $U^{\mathrm{sp}}(|x|)$ exists for these parameter values provided $\gamma < 0$. For $\gamma > 0$, the situation is slightly more complicated. For $0 < \gamma < 0.431$, there exist two unstable radial spots $U^{\mathrm{sp}}(|x|)$: the wider spot stabilizes at $\gamma = 0.431$ and merges and disappears with the second unstable radial spot at $\gamma = 0.653$ in a saddle-node bifurcation. We summarize these results in Table 2.

In Figure 3, we present numerical simulations for values of γ in the different regions shown in Table 2. In the top frame, we have $\gamma = 0.5$: we see that the front moves away from the spot, and no genuine interaction leading, for instance, to annihilation, repulsion, or soliton-like transmission occurs for this set of systems parameters, as was expected from the results for the single objects. We believe that stable fronts will always move away from stable spots (at least for $0 < \epsilon \ll 1$) but are not able to prove this: some analytical evidence is presented below. We remark that the front stops moving when it approaches the boundary: instead, it forms a stationary stable stripe $U^{\mathrm{st}}(x_1)$. This is expected as we use Neumann boundary conditions and, as we shall show in §2.2, the system exhibits stable stationary stripes for the parameter values used.

In the remaining frames of Figure 3, the radial spot is unstable, and the simulations therefore illustrate the interaction of a stable front (moving to the left or to the right) with an unstable spot. In all these cases, the unstable spot grows in diameter with a speed that increases as we decrease γ. The growth in diameter of the unstable spot continues until the spot comes close to the stable front. For small γ, front and spot do not collide, but they interact strongly and change their shape. For $\gamma \gg 1$, front and spot collide, and no patterns remains; see the bottom frame of Figure 3.

Figure 4 explores the situation where an unstable spot is sandwiched between two stable planar fronts that move towards the spot. Initially, the spots expands radially but its growth is eventually checked by the inwards moving fronts, who cause the spot to shrink in size until it disappears. The final pattern that emerges is a stationary

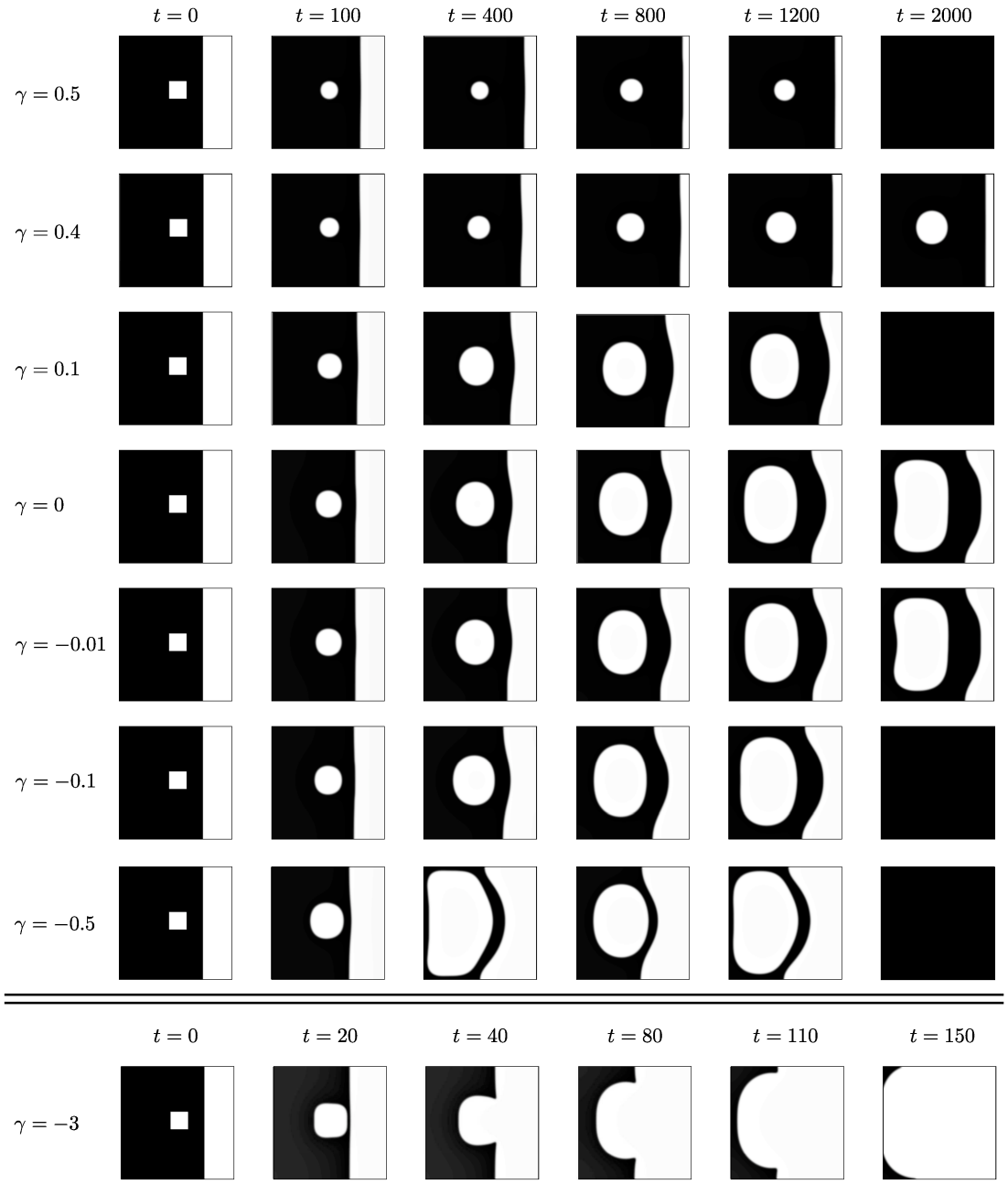

Figure 3. Shown are color plots of the u-component of solutions of (1.1) at different times for different values of the forcing parameter γ. The other parameters are fixed as in Table 1, and the initial condition consists in all cases of a square structure glued together with a stable front. The top frame illustrates the interaction of stable spots and stable planar travelling fronts. The spot structure evolves towards the stationary spot, while the front travels away from the spot and is slowed down when it approaches the boundary. In the other frames, the spot is unstable and grows in diameter until it begins to interact with the traveling front. For $|\gamma|$ large enough, the spot and front collide as illustrated in the bottom frame. See also Table 2.

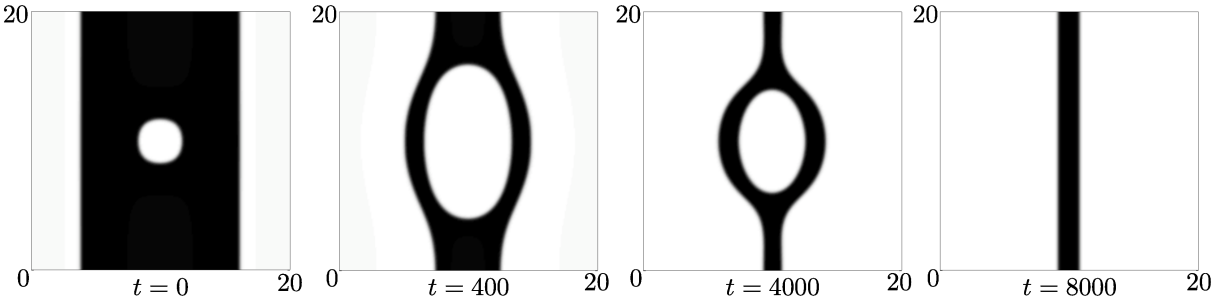

Figure 4. The time frames presented here illustrate the interaction of an unstable spot with two stable planar travelling fronts that move towards the spot from either side. After initially expanding, the spot is pushed back by the fronts until the spot disappears and the fronts merge to form a stationary stable stripe. We shall show in Lemma 2.1 below that (1.1) admits a stable stripe for the parameters in this simulation, which are given in Table 1.

stable stripe that consists of the two fronts that are glued together. The existence and stability of such stripe patterns will be studied in § 2.2 below.

In the remainder of this section, we discuss the conjecture mentioned in the beginning of this section:

Conjecture: *Stable planar travelling fronts always move away from stable stationary radial spots.*

We now try to prove the preceding statement. Since the spots in Theorem 1.3 asymptote to $U = U_*^-$ as $|x| \to \infty$, and the planar front profiles $U^{\mathrm{fr}}(x_1 - ct)$ we considered satisfy $U^{\mathrm{fr}}(x_1 - ct) \to U_*^{\pm}$ as $x_1 \to \pm\infty$, we need to place the front to the right of the spot. Thus, the speed c of the front $U^{\mathrm{fr}}(x_1 - ct)$ needs to be negative if the front is to move towards the spot. Theorem 1.1 shows that such fronts exist for $0 < \epsilon \ll 1$ if, and only if, $\gamma < 0$. Theorem 1.2 shows in addition that the resulting planar fronts are stable provided $\alpha + \frac{\beta}{D} < \frac{2\sqrt{2}}{3}$. In summary, the desired stable planar front exists if, and only if,

$$\gamma < 0 \qquad \text{and} \qquad \alpha + \frac{\beta}{D} < \frac{2\sqrt{2}}{3}. \tag{2.1}$$

From now on, we therefore assume that (2.1) is met. To prove the conjecture, we would then need to show that spots are unstable whenever (2.1) holds. The existence and stability properties of spots are given in Theorem 1.3, and we assume that $L = L_* > 0$ is a root of the function

$$R(L; \alpha, \beta, \gamma, D) = \frac{\sqrt{2}}{3L} + \alpha\Big(2LI_1(L)K_0(L) - 1\Big) + \beta\left(\frac{2L}{D} I_1\left(\frac{L}{D}\right) K_0\left(\frac{L}{D}\right) - 1\right) + \gamma$$

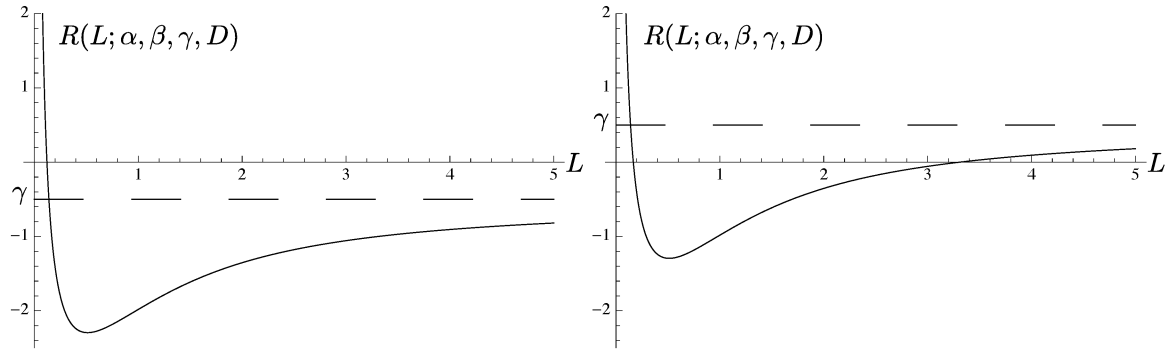

Figure 5. Plotted is the graph of $R(L;\alpha,\beta,\gamma,D)$ from (1.3) as a function of L for $\gamma<0$ in the left panel and for $\gamma>0$ in the right panel. Note that roots with negative slopes correspond to unstable spots, while roots with positive slopes give spots that are stable with respect to radial perturbations.

given in (1.3) that governs the existence of spots. We observe that its derivative $R_L(L_*;\alpha,\beta,\gamma,D)$ is proportional to the quantity $\lambda_0(L_*;\alpha,\beta,D)$ given in (1.4) that corresponds to the rightmost PDE eigenvalue of the spot belonging to a radial eigenfunction. More precisely, we have

$$R_L(L_*;\alpha,\beta,\gamma,D)=-\frac{\sqrt{2}}{3}\lambda_0(L_*;\alpha,\beta,D)\,, \tag{2.2}$$

and the spot is unstable with respect to radial perturbations if, and only if, the graph of $R(L;\alpha,\beta,\gamma,D)$ crosses zero with negative slope as L increases through L_*. As illustrated in Figure 5, we have

$$\lim_{L\downarrow 0} R(L;\alpha,\beta,\gamma,D)=\infty \quad\text{and}\quad \lim_{L\to\infty} R(L;\alpha,\beta,\gamma,D)=\gamma\,. \tag{2.3}$$

We can therefore label positive roots of R with increasing magnitude and conclude that roots of R with odd labels correspond to unstable spots, while spots corresponding to even-labelled roots are stable with respect to radial perturbations (though they could still be unstable with respect to nonradial perturbations). In particular, the conjecture is true if (2.1) is met and if $R(L;\alpha,\beta,\gamma,D)$ has at most one root or, slightly stronger, if $\lambda_0(L;\alpha,\beta,D)$ has no root. If α and β are both negative, we can use [6, Lemma 3.3] to conclude that $\lambda_0(L;\alpha,\beta,D)$ is positive for all $L>0$: this fact, together with (2.1) and (2.3), implies that $R(L;\alpha,\beta,\gamma,D)$ has a unique root, which then corresponds to an unstable spot. If, on the other hand, at least one of the parameters α and β is positive, we cannot explicitly determine the maximum number of crossings of $R(L;\alpha,\beta,\gamma,D)$, and the conjecture remains therefore unproven.

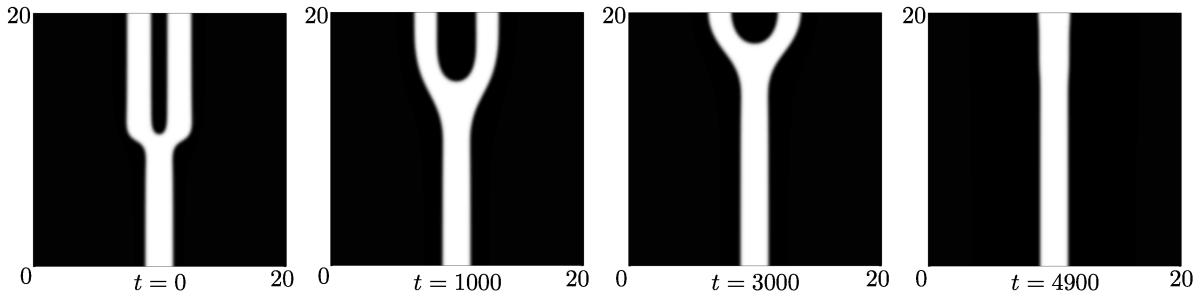

Figure 6. A defect is transported towards infinity, and a stable stationary planar stripe is formed. The system parameters are given in Table 1.

§ 2.2. Stripes

The solution shown in Figure 4 converges to a stationary stripe pattern that can be thought of as a bound state of two planar fronts. The existence and stability of 1D stripes has been analysed in [2, 3, 5], and the results obtained in these papers are summarized in Theorem 1.1. Our next result gives conditions under which planar stripes are stable with respect to 2D perturbations.

Lemma 2.1. *Fix $D > 1$, $\tau, \theta > 0$, $\alpha, \beta, \gamma \in \mathbb{R}$, and $k_* > 0$, and assume that there is a constant $L > 0$ such that $\alpha \mathrm{e}^{-2L} + \beta \mathrm{e}^{-2L/D} = \gamma$. Theorem 1.1 implies that (1.1) has a stationary stripe $U^{\mathrm{st}}(x_1)$ of width $2L$ for each $0 < \epsilon \ll 1$, and these stripes are stable with respect to perturbations whose transverse wave number k satisfies $|k| < k_*$ provided*

$$\lambda_k^{\pm}(L) = -k^2 - \frac{3\alpha}{\sqrt{2}} \left(\frac{1}{\sqrt{1+k^2}} - 1 + \mathrm{e}^{-2L} \mp \frac{1}{\sqrt{1+k^2}} \mathrm{e}^{-2\sqrt{1+k^2}L} \right) - \frac{3\beta}{\sqrt{2D}} \left(\frac{1}{\sqrt{1+k^2}} - 1 + \mathrm{e}^{-\frac{2L}{D}} \mp \frac{1}{\sqrt{1+k^2}} \mathrm{e}^{-2\sqrt{1+k^2}\frac{L}{D}} \right)$$

is strictly negative for all $|k| < k_*$.

We omit the proof as it is similar to the proof of Theorem 1.2 given in §3. We remark that results analogous to Lemma 2.1 hold for the existence and stability of planar N-fronts and N-stripes.

Stable stripes appeared in Figure 4 as the result of the interaction or two counter-propagating fronts. Figure 6 illustrates a different mechanism that leads to stripes: The initial condition consists of a defect between a stripe and a 2-stripe. As time increases, the defect moves towards infinity, thus leaving only the stable stationary stripe behind. Figure 7 indicates that stable stationary planar spots and stripes can coexist.

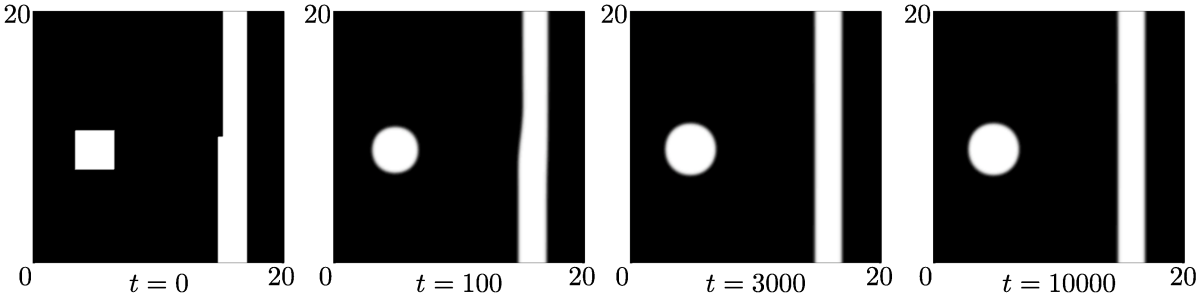

Figure 7. The coexistence of a stable stationary planar spot and stripe. The system parameters are given in Table 1.

§ 3. Planar travelling fronts

Our goal is to prove Theorem 1.2 which gives conditions under which the planar travelling front $U^{\mathrm{fr}}(x_1 - ct)$ of (1.1) guaranteed by Theorem 1.1 is spectrally stable with respect to perturbations that depend on (x_1, x_2). In fact, we will establish the following, slightly stronger result.

Theorem 3.1. *Fix $D > 1$, $\tau, \theta > 0$, and $\alpha, \beta, \gamma \in \mathbb{R}$ and pick any constant k_*, then the planar travelling front $U^{\mathrm{fr}}(x_1 - ct)$ of system (1.1) given in Theorem 1.1 is spectrally stable for all sufficiently small values of ϵ with respect to perturbations whose transverse wave number k satisfies $|k| < k_*$ provided*

$$\tilde{\lambda}(k) = \frac{3}{\sqrt{2}} \left(\alpha + \frac{\beta}{D} \right) \left(1 - \frac{1}{\sqrt{1 + k^2}} \right) - k^2 \leq 0 \tag{3.1}$$

for all $|k| < k_*$, and equality holds only for $k = 0$.

Theorem 1.2 is a consequence of Theorem 3.1, since

$$\alpha + \frac{\beta}{D} < \frac{2\sqrt{2}}{3} \tag{3.2}$$

implies (3.1). To see this, we first observe that $\tilde{\lambda}(0)$, which corresponds to the eigenvalue induced by translation of the front in the x_1-direction, vanishes. Moreover, it is obvious that for $\alpha + \frac{\beta}{D} < 0$ the eigenvalue $\tilde{\lambda}(k)$ is negative, and thus yield a stable travelling front. If $\alpha + \frac{\beta}{D} > 0$, we consider the second derivative

$$\tilde{\lambda}''(k) = -2 + \frac{3}{\sqrt{2}} \left(\alpha + \frac{\beta}{D} \right) \left(\frac{1}{(1 + k^2)\sqrt{1 + k^2}} - \frac{3k^2}{(1 + k^2)^2 \sqrt{1 + k^2}} \right)$$

of $\tilde{\lambda}(k)$: a calculation shows that $\tilde{\lambda}''(k) \leq 0$ and $\tilde{\lambda}(0) < 0$ whenever (3.2) holds, and the claim follows.

To prove Theorem 3.1, we need more detailed information about the profiles of the U^{fr} than provided by the existence results in [2, 3, 5], and we therefore focus first on the derivation of the relevant expansions.

Assuming that the front moves in the x_1-direction, we introduce the travelling coordinate $\eta = x_1 - \varepsilon^2 ct$ and write $U^{\mathrm{fr}}(x_1 - \varepsilon^2 ct) = U^{\mathrm{fr}}(\eta)$, where we also anticipate, with a slight abuse of notation, the scaling of the wave speed $\epsilon^2 c$. Recall also the rest states u_*^- and u_*^+ from (1.2). We now closely follow the analysis in [2, 3, 5] introduce the following slow regions $I_{\mathrm{s}}^{\pm}$ and the fast region I_{f} of the spatial variable η given by

$$I_{\mathrm{s}}^- = \{\eta \mid \eta \in \big(-\infty, -\sqrt{\epsilon}\big]\}\,, \quad I_{\mathrm{f}} = \{\eta \mid \eta \in \big(-\sqrt{\epsilon}, \sqrt{\epsilon}\big)\}\,, \quad I_{\mathrm{s}}^+ = \{\eta \mid \eta \in \big[\sqrt{\epsilon}, \infty\big)\}\,.$$

The idea is now that, in the fast field I_{f}, the u-component of the front profile will jump from u_*^- to u_*^+, see (1.2), while the slow (v, w)-components of the profile are, to leading order, constant: due to the specific scaling of the diffusion coefficients in (1.1), the region I_{f} is too small for the slow components to change significantly. In contrast, the slow (v, w)-components are gradually changing in the slow regions $I_{\mathrm{s}}^{\pm}$, while the fast u-component will already have attained its asymptotic state and will therefore not change much. To capture the fast jump in the u-component, it is convenient to use the fast variable $\xi = \frac{\eta}{\epsilon}$. In the following lemma, we state the desired expansion of the front profiles that we shall then exploit in the stability proof.

Lemma 3.2. *Writing*

$$\begin{aligned} u^{\mathrm{fr}}(\xi) &= u_0^{\mathrm{fr}}(\xi) + \epsilon u_1^{\mathrm{fr}}(\xi) + \epsilon u_2^{\mathrm{fr}}(\xi) + \mathcal{O}(\epsilon^3)\,, \\ v^{\mathrm{fr}}(\eta) &= v_0^{\mathrm{fr}}(\eta) + \mathcal{O}(\epsilon)\,, \\ w^{\mathrm{fr}}(\eta) &= w_0^{\mathrm{fr}}(\eta) + \mathcal{O}(\epsilon) \end{aligned} \tag{3.3}$$

for the profile $U^{\mathrm{fr}} = (u^{\mathrm{fr}}, v^{\mathrm{fr}}, w^{\mathrm{fr}})$ of the planar front, we have

$$u_0^{\mathrm{fr}}(\xi) = \tanh\left(\frac{\xi}{\sqrt{2}}\right), \tag{3.4}$$

and

$$v^{\mathrm{fr}}(\eta) = \begin{cases} \mathrm{e}^{\eta} - 1 & \text{in } I_{\mathrm{s}}^-, \\ 0 & \text{in } I_{\mathrm{f}}, \\ -\mathrm{e}^{-\eta} + 1 & \text{in } I_{\mathrm{s}}^+, \end{cases} \qquad w^{\mathrm{fr}}(\eta) = \begin{cases} \mathrm{e}^{\frac{\eta}{D}} - 1 & \text{in } I_{\mathrm{s}}^-, \\ 0 & \text{in } I_{\mathrm{f}}, \\ -\mathrm{e}^{-\frac{\eta}{D}} + 1 & \text{in } I_{\mathrm{s}}^+. \end{cases} \tag{3.5}$$

Furthermore, the first-order correction $u_1^{\mathrm{fr}}(\xi)$ is an even function in I_{f}, and its derivative obeys the relation

$$\mathcal{L}(u_1^{\mathrm{fr}})_\xi := ((u_1^{\mathrm{fr}})_\xi)_{\xi\xi} + (u_1^{\mathrm{fr}})_\xi - 3(u_0^{\mathrm{fr}})^2 (u_1^{\mathrm{fr}})_\xi = -\frac{c}{\sqrt{2}}\psi_\xi + 3\sqrt{2} u_0^{\mathrm{fr}} u_1^{\mathrm{fr}} \psi\,, \tag{3.6}$$

where ψ is defined as

$$\psi := \operatorname{sech}^2\left(\frac{\xi}{\sqrt{2}}\right) = \sqrt{2}(u_0^{\mathrm{fr}})_\xi. \tag{3.7}$$

Finally, the second-order correction $u_2^{\mathrm{fr}}(\xi)$ in I_{f} satisfies the integral relation

$$\begin{aligned} 0 = 2\sqrt{2}\left(\alpha + \frac{\beta}{D}\right) - c\int (u_1^{\mathrm{fr}})_{\xi\xi}\psi d\xi + 3\sqrt{2}\int u_0^{\mathrm{fr}} u_2^{\mathrm{fr}}\psi^2 d\xi \\ + \frac{3}{\sqrt{2}}\int (u_1^{\mathrm{fr}})^2\psi^2 d\xi + 6\int u_0^{\mathrm{fr}} u_1^{\mathrm{fr}}(u_1^{\mathrm{fr}})_\xi \psi d\xi\,. \end{aligned} \tag{3.8}$$

Proof. Equations (3.4) and (3.5) follow from an analysis similar to the one in [2] and will be omitted. To prove the second part of the lemma, we look at the fast u-equation in the fast variable ξ:

$$0 = u_{\xi\xi} + u - u^3 - \epsilon(\alpha v + \beta w + \gamma - c u_\xi)\,. \tag{3.9}$$

Substituting the expansions for U^{fr} and using that

$$0 = (u_0^{\mathrm{fr}})_{\xi\xi} + u_0^{\mathrm{fr}} - (u_0^{\mathrm{fr}})^3,$$

and that the slow components vanish to leading order in the fast field I_{f} due to (3.5), we get

$$\begin{aligned} 0 &= \epsilon\left((u_1^{\mathrm{fr}})_{\xi\xi} + u_1^{\mathrm{fr}} - 3(u_0^{\mathrm{fr}})^2 u_1^{\mathrm{fr}} - \gamma + c(u_0^{\mathrm{fr}})_\xi\right) + \mathcal{O}(\epsilon^2) \\ &= \epsilon\left(\mathcal{L}u_1^{\mathrm{fr}} - \gamma + \frac{c}{\sqrt{2}}\psi\right) + \mathcal{O}(\epsilon^2)\,, \end{aligned} \tag{3.10}$$

where $\mathcal{L}$ and ψ are defined in (3.6) and (3.7), respectively. Theorem 1.1 shows that $\gamma = \frac{\sqrt{2}}{3}c$ (recall that we rescaled the wave speed by ϵ^2 in this section), and we see that $u_1^{\mathrm{fr}}(\xi)$ is determined by the equation

$$\mathcal{L}u_1^{\mathrm{fr}} = \sqrt{2}c\left(\frac{1}{3} - \frac{1}{2}\psi\right)\,. \tag{3.11}$$

The right-hand side of (3.11) is even. Since the operator $\mathcal{L}$ respects the parity of a function, we split u_1^{fr} into its even and odd parts, given by $u_1^{\mathrm{fr,e}}$ and $u_1^{\mathrm{fr,o}}$, respectively, and find that

$$\mathcal{L}u_1^{\mathrm{fr,e}} = \sqrt{2}c\left(\frac{1}{3} - \frac{1}{2}\psi\right)\,, \qquad \mathcal{L}u_1^{\mathrm{fr,o}} = 0\,.$$

In particular, the odd part $u_1^{\mathrm{fr,o}}$ lies in the kernel of $\mathcal{L}$, which is, however, spanned by the even function $(u_0^{\mathrm{fr}})_\xi$. Thus, $u_1^{\mathrm{fr,o}} = 0$, and u_1^{fr} is even in I_{f} as claimed.

To obtain the relations (3.6) and (3.8), we substitute the front profile $U^{\rm fr}$ into (3.9) and differentiate the resulting equation once with respect to the fast variable ξ and obtain

$$0 = u^{\rm fr}_{\xi\xi\xi} + u^{\rm fr}_{\xi} - 3(u^{\rm fr})^2 u^{\rm fr}_{\xi} - \epsilon(\alpha v^{\rm fr}_{\xi} + \beta w^{\rm fr}_{\xi} - c u^{\rm fr}_{\xi\xi})\,.$$

Substituting the leading order expressions (3.5) for the slow components $(v^{\rm fr}, w^{\rm fr})$ and using the regular expansion (3.3), we arrive at

$$\begin{aligned} 0 = {} & \mathcal{L}(u^{\rm fr}_0)_\xi + \epsilon\left(\mathcal{L}(u^{\rm fr}_1)_\xi + c(u^{\rm fr}_0)_{\xi\xi} - 6u^{\rm fr}_0 u^{\rm fr}_1 (u^{\rm fr}_0)_\xi\right) \\ & + \epsilon^2\Big(\mathcal{L}(u^{\rm fr}_2)_\xi - \alpha - \frac{\beta}{D} + c(u^{\rm fr}_1)_{\xi\xi} - 6u^{\rm fr}_0 u^{\rm fr}_2 (u^{\rm fr}_0)_\xi \\ & - 3(u^{\rm fr}_1)^2 (u^{\rm fr}_0)_\xi - 6u^{\rm fr}_0 u^{\rm fr}_1 (u^{\rm fr}_1)_\xi\Big)\,. \end{aligned} \tag{3.12}$$

Since $(u^{\rm fr}_0)_\xi$ is in the kernel of $\mathcal{L}$, the $\mathcal{O}(1)$-terms in (3.12) vanish, while the equations at order $\mathcal{O}(\epsilon)$ give (3.6) upon using (3.7). To derive the integral relation (3.8), we consider the $\mathcal{O}(\epsilon^2)$-terms in (3.12). Since ψ is in the kernel of $\mathcal{L}$, the Fredholm property gives

$$\begin{aligned} 0 = {} & \langle \psi, \mathcal{L}(u^{\rm fr}_2)_\xi\rangle \\ = {} & \langle \psi, \alpha + \frac{\beta}{D} - c(u^{\rm fr}_1)_{\xi\xi} + 6u^{\rm fr}_0 u^{\rm fr}_2 (u^{\rm fr}_0)_\xi + 3(u^{\rm fr}_1)^2 (u^{\rm fr}_0)_\xi + 6u^{\rm fr}_0 u^{\rm fr}_1 (u^{\rm fr}_1)_\xi\rangle \\ = {} & \left(\alpha + \frac{\beta}{D}\right)\int \psi d\xi - c\int (u^{\rm fr}_1)_{\xi\xi}\psi d\xi + 3\sqrt{2}\int u^{\rm fr}_0 u^{\rm fr}_2 \psi^2 d\xi \\ & + \frac{3}{\sqrt{2}}\int (u^{\rm fr}_1)^2\psi^2 d\xi + 6\int u^{\rm fr}_0 u^{\rm fr}_1 (u^{\rm fr}_1)_\xi \psi d\xi \\ = {} & 2\sqrt{2}\left(\alpha + \frac{\beta}{D}\right) - c\int (u^{\rm fr}_1)_{\xi\xi}\psi d\xi + 3\sqrt{2}\int u^{\rm fr}_0 u^{\rm fr}_2 \psi^2 d\xi \\ & + \frac{3}{\sqrt{2}}\int (u^{\rm fr}_1)^2\psi^2 d\xi + 6\int u^{\rm fr}_0 u^{\rm fr}_1 (u^{\rm fr}_1)_\xi \psi d\xi\,, \end{aligned} \tag{3.13}$$

which completes the proof. □

With this lemma in hand, we can complete the proof of Theorem 3.1. We linearize (1.1) in the travelling coordinates around the planar front $U^{\rm fr}(\eta)$ and determine the spectrum of the resulting planar PDE operator whose coefficients depend only on η. The spectrum consists entirely of essential spectrum: specifically, it consists of the essential spectrum of the background states and contributions from the front interface. We focus first on the background states.

Lemma 3.3. *Fix any χ with $\max\{-2, -\frac{1}{\tau}, -\frac{1}{\theta}\} < \chi < 0$, then, for all sufficiently small ϵ, the essential spectrum of the background states of the travelling planar front lies in the half plane $\{\lambda :\ \mathrm{Re}\,\lambda < \chi\}$.*

Proof. Using the Fourier transform with spatial wave numbers (k, n) in the (η, x_2)-directions, the eigenvalue problem for the PDE operator linearized around the background states becomes

$$\begin{aligned} (\lambda - \epsilon^2 cik)u &= -\epsilon^2(k^2+n^2)u + u(1-3(u_*^{\pm})^2) - \epsilon(\alpha v + \beta w)\,, \\ \tau(\lambda - \epsilon^2 cik)v &= \qquad (k^2+n^2)v + u - v\,, \\ \theta(\lambda - \epsilon^2 cik)w &= D^2(k^2+n^2)w + u - w\,, \end{aligned} \tag{3.14}$$

where $u_*^{\pm}$ are the background states as defined in (1.2). Replacing λ by $\lambda + \epsilon^2 cik$ does not change the real part of λ, and it therefore suffices to analyse the reduced eigenvalue problem

$$\begin{pmatrix} 0 \\ 0 \\ 0 \end{pmatrix} = \begin{pmatrix} -\epsilon^2\ell^2 - 2 + \mathcal{O}(\epsilon) - \lambda & -\epsilon\alpha & -\epsilon\beta \\ 1 & -\ell^2 - 1 - \tau\lambda & 0 \\ 1 & 0 & -D^2\ell^2 - 1 - \theta\lambda \end{pmatrix} \begin{pmatrix} u \\ v \\ w \end{pmatrix}, \tag{3.15}$$

where $\ell^2 := k^2 + n^2$. The real part of the eigenvalues λ is determined by the zeros of

$$\begin{aligned} 0 &= (-\epsilon^2\ell^2 - 2 + \mathcal{O}(\epsilon) - \lambda)(-\ell^2 - 1 - \tau\lambda)(-D^2\ell^2 - 1 - \theta\lambda) \\ &\quad + \epsilon\alpha(-D^2\ell^2 - 1 - \theta\lambda) + (\epsilon\beta(-\ell^2 - 1 - \tau\lambda)) \\ &= (-\epsilon^2\ell^2 - 2 - \lambda)(-\ell^2 - 1 - \tau\lambda)(-D^2\ell^2 - 1 - \theta\lambda) + \mathcal{O}(\epsilon)\,, \end{aligned}$$

and a closer inspection shows that the rightmost part of the essential spectrum occurs for $(k, n) = 0$, which proves the claim. □

To analyse the contributions from the front interface, we consider the eigenvalue problem

$$\begin{aligned} \lambda u &= \quad \epsilon^2\Delta u + u(1-3(u^{\mathrm{fr}}(\eta,\epsilon))^2) - \epsilon(\alpha v + \beta w) + \epsilon^2 c u_\eta\,, \\ \tau\lambda v &= \qquad \Delta v + u - v + \epsilon^2\tau c v_\eta\,, \\ \theta\lambda w &= D^2\Delta w + u - w + \epsilon^2\theta c w_\eta\,. \end{aligned} \tag{3.16}$$

Applying the Fourier transform in the x_2-direction, that is, setting

$$(u, v, w)(\eta, x_2) = (u, v, w)(\eta)\mathrm{e}^{ikx_2}\,, \quad k \in \mathbb{R},$$

in (3.16), we arrive at the system

$$\begin{aligned} 0 &= \quad \epsilon^2 u_{\eta\eta} + u(1-3(u^{\mathrm{fr}}(\eta,\epsilon))^2 - \lambda - \epsilon^2 k^2) - \epsilon(\alpha v + \beta w) + \epsilon^2 c u_\eta\,, \\ 0 &= \qquad v_{\eta\eta} + u - v(1 + \tau\lambda + k^2) + \epsilon^2\tau c v_\eta\,, \\ 0 &= D^2 w_{\eta\eta} + u - w(1 + \theta\lambda + k^2) + \epsilon^2\theta c w_\eta\,. \end{aligned} \tag{3.17}$$

In the fast scaling $\xi = \frac{\eta}{\epsilon}$, the u-equation in (3.17) becomes

$$0 = u_{\xi\xi} + u(1 - 3(u^{\mathrm{fr}}(\xi,\epsilon))^2 - \lambda - \epsilon^2 k^2) - \epsilon(\alpha v + \beta w - c u_\xi)\,,$$

and therefore, since we assumed that k is bounded independently of ϵ by some constant k_*, we obtain

$$0 = u_{\xi\xi} + u(1 - 3(u_0^{\mathrm{fr}})^2 - \lambda)\,, \tag{3.18}$$

where u_0^{fr} is the leading order term of the u^{fr}-profile given in (3.4). It was shown in [3] that the eigenvalues of (3.18) are given by

$$\lambda_1 = 0\,, \quad \lambda_2 = -\frac{3}{2}\,.$$

Thus, the only possible unstable contributions for $0 < \epsilon \ll 1$ arise from λ_1. We therefore expand λ_1 as

$$\lambda = \epsilon\hat{\lambda}$$

in the following. We also need to rescale the slow components (v, w), since solving the leading parts of the slow equations of (3.17) in the regions $I_{\mathrm{s}}^{\pm}$, and matching them over the fast region I_{f} gives, to leading order, $(v, w) = 0$. Therefore, we write

$$(v, w) = \epsilon(\hat{v}, \hat{w})\,,$$

and substitution into (3.17) gives

$$\begin{aligned}
0 = {} & \epsilon^2 u_{\eta\eta} + u(1 - 3(u^{\mathrm{fr}}(\eta,\epsilon))^2) - \epsilon u\hat{\lambda} - \epsilon^2(\alpha\hat{v} + \beta\hat{w} - c u_\eta - k^2 u)\,,\\
0 = {} & \hat{v}_{\eta\eta} + \tfrac{u}{\epsilon} - \hat{v}(1 + k^2) - \epsilon\tau\hat{\lambda}\hat{v} + \epsilon^2\tau c\hat{v}_\eta\,,\\
0 = {} & D^2\hat{w}_{\eta\eta} + \tfrac{u}{\epsilon} - \hat{w}(1 + k^2) - \epsilon\theta\hat{\lambda}\hat{w} + \epsilon^2\theta c\hat{w}_\eta\,.
\end{aligned} \tag{3.19}$$

To analyse this equation, we rewrite the u-equation in the fast variable ξ in the fast region I_{f} and obtain

$$0 = u_{\xi\xi} + u(1 - 3(u^{\mathrm{fr}})^2) - \epsilon(\hat{\lambda}u - c u_\xi) - \epsilon^2(\alpha\hat{v} + \beta\hat{w} + k^2 u)\,. \tag{3.20}$$

Substituting regular expansions for u^{fr} and u, this equation becomes

$$\begin{aligned}
\mathcal{O}(\epsilon^2) = {} & (u_0)_{\xi\xi} + u_0\left(1 - 3(u_0^{\mathrm{fr}})^2\right)\\
& + \epsilon\left((u_1)_{\xi\xi} + u_1\left(1 - 3(u_0^{\mathrm{fr}})^2\right) - u_0(\hat{\lambda} + 6u_0^{\mathrm{fr}}u_1^{\mathrm{fr}}) + c(u_0)_\xi\right)\\
=: {} & \mathcal{L}u_0 + \epsilon\left(\mathcal{L}u_1 - u_0(\hat{\lambda} + 6u_0^{\mathrm{fr}}u_1^{\mathrm{fr}}) + c(u_0)_\xi\right)\,.
\end{aligned}$$

To leading order, we therefore conclude that $\mathcal{L}u_0 = 0$, which implies that u_0 is given by

$$u_0 = \tilde{C}\frac{d}{d\xi}u_0^{\mathrm{fr}} = \frac{\tilde{C}}{\sqrt{2}}\mathrm{sech}^2\left(\frac{\xi}{\sqrt{2}}\right) =: C\psi$$

due to (3.3), (3.7), and the results in [3]. At order $\mathcal{O}(\epsilon)$, the equation above becomes

$$\mathcal{L}u_1 = C(\hat{\lambda}\psi + 6u_0^{\mathrm{fr}}u_1^{\mathrm{fr}}\psi - c\psi_\xi)\,.$$

Using that $u_0^{\mathrm{fr}}u_1^{\mathrm{fr}}$ and $\psi\psi_\xi$ are odd functions in the fast region I_{f} by Lemma 3.2, and that ψ is in the kernel of $\mathcal{L}$, the Fredholm property gives

$$0 = \langle \psi, \mathcal{L}u_1\rangle = C\left(\hat{\lambda}\int \psi^2 d\xi - c\int \psi\psi_\xi d\xi + 6\int u_0^{\mathrm{fr}}u_1^{\mathrm{fr}}\psi^2 d\xi\right) = \frac{4\sqrt{2}}{3}C\hat{\lambda}$$

and we conclude that, to leading order, $\hat{\lambda} = 0$.

Thus, we need to rescale once more and set

$$\hat{\lambda} = \epsilon\tilde{\lambda}\,,$$

which transforms (3.19) into

$$\begin{aligned} 0 =&\quad \epsilon^2 u_{\eta\eta} + u(1 - 3(u^{\mathrm{fr}})^2) - \epsilon^2(\alpha\hat{v} + \beta\hat{w} - cu_\eta + u(\tilde{\lambda} + k^2))\,,\\ 0 =&\quad \hat{v}_{\eta\eta} + \tfrac{u}{\epsilon} - \hat{v}(1+k^2) - \epsilon^2\tau(\tilde{\lambda}\hat{v} + c\hat{v}_\eta)\,,\\ 0 =& D^2\hat{w}_{\eta\eta} + \tfrac{u}{\epsilon} - \hat{w}(1+k^2) - \epsilon^2\theta(\tilde{\lambda}\hat{w} + c\hat{w}_\eta)\,. \end{aligned} \tag{3.21}$$

In the slow regions $I_{\mathrm{s}}^{\pm}$, the fast component u is small, and the slow equations therefore decouple to leading order in the slow regions where they are given by

$$\begin{aligned} \mathcal{O}(\epsilon^2) =&\quad \hat{v}_{\eta\eta} - \hat{v}(1+k^2)\,,\\ \mathcal{O}(\epsilon^2) =& D^2\hat{w}_{\eta\eta} - \hat{w}(1+k^2)\,. \end{aligned} \tag{3.22}$$

Since the components should be bounded at infinity, we obtain the leading order expressions

$$\hat{v}(\eta) = \begin{cases} A_v \mathrm{e}^{\sqrt{1+k^2}\eta} & \text{in } I_{\mathrm{s}}^-,\\ B_v \mathrm{e}^{-\sqrt{1+k^2}\eta} & \text{in } I_{\mathrm{s}}^+, \end{cases} \qquad \hat{w}(\eta) = \begin{cases} A_w \mathrm{e}^{\sqrt{1+k^2}\frac{\eta}{D}} & \text{in } I_{\mathrm{s}}^-,\\ B_w \mathrm{e}^{-\sqrt{1+k^2}\frac{\eta}{D}} & \text{in } I_{\mathrm{s}}^+ \end{cases} \tag{3.23}$$

of the slow components $\hat{v}$ and $\hat{w}$. In the new scaling, the slow components taken across I_{f} agree, but their derivatives do not. This can be seen best by working in the fast variable ξ for which $|\xi| \leq \frac{1}{\sqrt{\epsilon}}$ in I_{f}. In this region, the $\hat{v}$-equation, for instance, becomes

$$\hat{v}_{\xi\xi} = -\epsilon u + \epsilon^2\hat{v}(1+k^2) + \epsilon^3\tau c\hat{v}_\xi + \epsilon^4\tau\tilde{\lambda}\hat{v}\,,$$

or, equivalently,

$$\hat{v}_\xi = \epsilon\hat{q}\,, \qquad \hat{q}_\xi = -u + \epsilon\hat{v}(1+k^2) + \mathcal{O}(\epsilon^3)\,.$$

Therefore, the change of $\hat{v}$ and $\hat{q} = v_\eta$ across $I_{\rm f}$ is, to leading order, given by

$$\Delta_f \hat{v} := \int_{I_f} \hat{v}_\xi d\xi = \epsilon \int_{-\infty}^{\infty} \hat{q} d\xi = \mathcal{O}(\sqrt{\epsilon}) \,,$$
$$\Delta_f \hat{q} := \int_{I_f} \hat{q}_\xi d\xi = -\int_{-\infty}^{\infty} u_0 d\xi = -C \int_{-\infty}^{\infty} \psi d\xi = -2\sqrt{2}C + \mathcal{O}(\sqrt{\epsilon}) \,.$$

Substituting (3.23), we find that the coefficients A_v and B_v need to satisfy the system

$$A_v = B_v \qquad \text{and} \qquad \sqrt{1+K^2} A_v - 2\sqrt{2}C = -\sqrt{1+K^2} B_v \,,$$

so that

$$A_v = B_v = \sqrt{\frac{2}{1+k^2}} C \,.$$

Similarly, we obtain

$$A_w = B_w = \sqrt{\frac{2}{1+k^2}} \frac{C}{D} \,.$$

We substitute the resulting expressions (3.23) into the u-equation to get

$$u_{\xi\xi} + u(1 - 3(u^{\rm fr})^2) = -\epsilon c u_\xi + \epsilon^2 (\alpha A_v + \beta B_w + u(\tilde{\lambda} + k^2)) \,.$$

Expanding $u^{\rm fr}$ and u in ϵ, we obtain the equation

$$\mathcal{L} u_1 = -C \left(c\psi_\xi - 6 u_0^{\rm fr} u_1^{\rm fr} \psi \right) \tag{3.24}$$

at $\mathcal{O}(\epsilon)$. Note that the right-hand side of (3.24) is $\sqrt{2}C$ times the right-hand side of (3.6), and since the null space of $\mathcal{L}$ is spanned by ψ, we can conclude that

$$u_1 = \sqrt{2} C (u_1^{\rm fr})_\xi + K\psi \tag{3.25}$$

for some undetermined constant K. At $\mathcal{O}(\epsilon^2)$, we then have

$$\begin{aligned} \mathcal{L} u_2 &= (\alpha A_v + \beta A_w + u_0(\tilde{\lambda} + k^2)) - c(u_1)_\xi + 6 u_0 u_0^{\rm fr} u_2^{\rm fr} + 6 u_1 u_0^{\rm fr} u_1^{\rm fr} + 3 u_0 (u_1^{\rm fr})^2 \\ &= (\alpha A_v + \beta A_w + C\psi(\tilde{\lambda} + k^2)) - c(u_1)_\xi + 6 C\psi u_0^{\rm fr} u_2^{\rm fr} + 6 u_1 u_0^{\rm fr} u_1^{\rm fr} + 3 C\psi (u_1^{\rm fr})^2 \,. \end{aligned}$$

Using again the Fredholm property, we get

$$\begin{aligned}
0 &= (\alpha A_v + \beta A_w)\int \psi d\xi + C(\tilde{\lambda}+k^2)\int \psi^2 d\xi - c\int (u_1)_\xi \psi d\xi + 6C\int u_0^{\mathrm{fr}} u_2^{\mathrm{fr}} \psi^2 d\xi \\
&\quad +6\int u_1 u_0^{\mathrm{fr}} u_1^{\mathrm{fr}} \psi d\xi + 3C\int (u_1^{\mathrm{fr}})^2 \psi^2 d\xi \\
&= \frac{4}{\sqrt{1+k^2}} C\left(\alpha + \frac{\beta}{D}\right) + \frac{4\sqrt{2}}{3} C(\tilde{\lambda}+k^2) - c\int (\sqrt{2}C(u_1^{\mathrm{fr}})_\xi + K\psi)_\xi \psi d\xi \\
&\quad +6C\int u_0^{\mathrm{fr}} u_2^{\mathrm{fr}} \psi^2 d\xi + 6\int (\sqrt{2}C(u_1^{\mathrm{fr}})_\xi + K\psi) u_0^{\mathrm{fr}} u_1^{\mathrm{fr}} \psi d\xi + 3C\int (u_1^{\mathrm{fr}})^2 \psi^2 d\xi \\
&= \frac{4}{\sqrt{1+k^2}} C\left(\alpha + \frac{\beta}{D}\right) + \frac{4\sqrt{2}}{3} C(\tilde{\lambda}+k^2) - \sqrt{2}cC\int (u_1^{\mathrm{fr}})_{\xi\xi} \psi d\xi + 6C\int u_0^{\mathrm{fr}} u_2^{\mathrm{fr}} \psi^2 d\xi \\
&\quad +6\sqrt{2}C\int (u_1^{\mathrm{fr}})_\xi u_0^{\mathrm{fr}} u_1^{\mathrm{fr}} \psi d\xi + 3C\int (u_1^{\mathrm{fr}})^2 \psi^2 d\xi \\
&= 4C\left(\frac{1}{\sqrt{1+k^2}}\left(\alpha + \frac{\beta}{D}\right) + \frac{\sqrt{2}}{3}(\tilde{\lambda}+k^2) - \left(\alpha + \frac{\beta}{D}\right)\right),
\end{aligned}$$

and we find that the scaled eigenvalue $\tilde{\lambda}$ is given by

$$\tilde{\lambda}(k) = \frac{3}{\sqrt{2}}\left(\alpha + \frac{\beta}{D}\right)\left(1 - \frac{1}{\sqrt{1+k^2}}\right) - k^2 \tag{3.26}$$

as claimed. This completes the proof of Theorem 3.1. ■

References

[1] Abramowitz, M. and Stegun, I. A., *Handbook of Mathematical Functions with Formulas, Graphs, and Mathematical Tables*, NIST, 1964.

[2] Doelman, A., van Heijster, P. and Kaper, T. J., Pulse dynamics in a three-component system: existence analysis, *J. Dynam. Differ. Eqns.*, **21** (2009), 73–115.

[3] van Heijster, P., Doelman, A. and Kaper, T. J., Pulse dynamics in a three-component system: stability and bifurcations, *Physica D*, **237** (2008), 3335–3368.

[4] van Heijster, P., Doelman, A., Kaper, T. J., Nishiura, Y. and Ueda, K.-I., Pinned fronts in heterogeneous media of jump type, *Nonlinearity*, **24** (2011), 127–157.

[5] van Heijster, P., Doelman, A., Kaper, T. J. and Promislow, K., Front interactions in a three-component system, *SIAM J. Appl. Dyn. Syst.*, **9** (2010), 292–332.

[6] van Heijster, P. and Sandstede, B., Planar radial spots in a three-component Fitzhugh–Nagumo system, *J. Nonlin. Sci.*, **21** (2011), 705–745.

[7] Kapitula, T., Multidimensional stability of planar travelling waves, *Trans. Amer. Math. Soc.*, **349** (1997), 257–269.

[8] Nishiura, Y., Teramoto, T. and Ueda, K.-I., Dynamic transitions through scattors in dissipative systems, *Chaos*, **13** (2003), 962–972.

[9] Nishiura, Y., Teramoto, T. and Ueda, K.-I., Scattering of traveling spots in dissipative systems, *Chaos*, **15** (2005), 047509.

[10] Or-Guil, M., Bode, M., Schenk, C.-P. and Purwins, H. G., Spot bifurcations in three-component reaction-diffusion systems: The onset of propagation, *Phys. Rev. E (6)*, **57** (1998), 6432–6437.

[11] Schenk, C.-P., Or-Guil, M., Bode, M. and Purwins, H. G., Interacting pulses in three-component reaction-diffusion systems on two-dimensional domains, *Phys. Rev. Lett.*, **78** (1997), 3781–3784.

[12] Vanag, V. K. and Epstein, I. R., Localized patterns in reaction-diffusion systems, *Chaos*, **17** (2007), 037110.

[13] Yuan, X., Teramoto, T. and Nishiura, Y., Heterogeneity-induced defect bifurcation and pulse dynamics for a three-component reaction-diffusion system, *Phys. Rev. E*, **75** (2007), 036220.